NANO LETTERS

2007
Vol. 7, No. 6
1626−1630

Bound Excitons in Metallic Single-Walled Carbon Nanotubes

Jack Deslippe,[†,‡] Catalin D. Spataru,[§] David Prendergast,[||] and Steven G. Louie*[,†,‡]

Department of Physics, University of California, Berkeley, Berkeley, California 94720, Materials Sciences Division, Lawrence Berkeley National Laboratory, Berkeley, California 94720, Center for Integrated Science and Engineering and Center for Electron Transport in Molecular Nanostructures, Columbia University, New York, New York 10027, and Chemical Sciences Division, Lawrence Berkeley National Laboratory, Berkeley, California 94720

Received March 12, 2007; Revised Manuscript Received April 24, 2007

ABSTRACT

We extend previous ab initio calculations on excitonic effects in metallic single-walled carbon nanotubes to more experimentally realizable larger diameter tubes. Our calculations predict bound exciton states in both the (10,10) and (12,0) tubes with binding energies of approximately 50 meV providing experimentally verifiable changes to the absorption line shape in each case. The second and third van Hove singularities in the joint density of states also give rise to a single optically active bound or resonant excitonic state.

Single-walled carbon nanotubes (SWCNTs) are quasi-1D structures made by rolling up graphene strips. The SWCNTs can be either metallic or semiconducting depending sensitively on the tube diameter and chiral angle.[1−3] Additionally, recent ab initio calculations[4,5] using the GW−Bethe−Salpeter equation (GW-BSE) technique[6−8] have predicted that excitonic effects are dominant in the optical properties of single-walled carbon nanotubes due to enhanced electron−electron interactions in quasi-1D materials. This was first examined in a **k·p** study, employing different strengths of a model electron−hole interaction on semiconducting SWCNTs.[9] The ab initio calculations showed the existence of discrete strongly bound exciton states below the two-particle continuum. Interestingly, these calculations also predicted that bound exciton states exist and can strongly affect the optical spectrum of metallic SWCNTs.[4,5] However, the previous ab initio calculations on metallic tubes were limited to tubes with small diameter, (3,3) and (5,0), and the analysis was only done for excitons associated with the first peak in the absorption spectrum. We present here ab initio calculations showing the existence of excitons in larger metallic SWCNTs that are experimentally viable, the (10,10) and (12,0) tubes, together with predicted features that are experimentally verifiable.

We find that optical absorption spectra of both the (10,10) and (12,0) tubes are dictated by bound exciton states with binding energies of 50 meV each. Moreover, the second and third optical peaks are also composed of narrow resonant exciton states with similar binding energies. Unlike semiconducting nanotubes, where higher energy bound exciton states exist, we find that metallic tubes possess only a single optically bright bound or resonant exciton state per van Hove singularity in the joint density of states (JDOS) because of metallic screening. The bound or resonant exciton state steals approximately 50% of the optical oscillator strength from the continuum part of the transition for the tubes studied. Thus, the peak in the optical absorption spectrum is derived predominantly from one Lorentzian and acquires a highly symmetric line shape, which is very different from that of an independent particle picture. These are concrete theoretical predictions that can be tested by experiment.

The excitonic picture for the optical spectra of semiconducting tubes has recently been confirmed by experiments using two-photon photoluminescence spectroscopy techniques.[10,11] However, because metallic tubes do not luminesce, this particular experimental technique is not applicable in the metallic case. The signature of excitonic effects in metallic tubes should however be seen, as discussed below, in other (such as absorption) measurements.

To compute the optical properties of metallic tubes from first-principles, we use the method of Rohlfing and Louie.[6] We treat the ground state within ab initio Kohn−Sham density functional theory (DFT) with a plane wave basis within the local density approximation (LDA) for the

* Corresponding author. E-mail: sglouie@uclink.berkeley.edu.
[†] Department of Physics, University of California at Berkeley.
[‡] Material Sciences Division, Lawrence Berkeley National Laboratory.
[§] Center for Integrated Science and Engineering and Center for Electron Transport in Molecular Nanostructures, Columbia University.
[||] Chemical Sciences Division, Lawrence Berkeley National Laboratory.

10.1021/nl070577f CCC: $37.00
Published on Web 05/18/2007

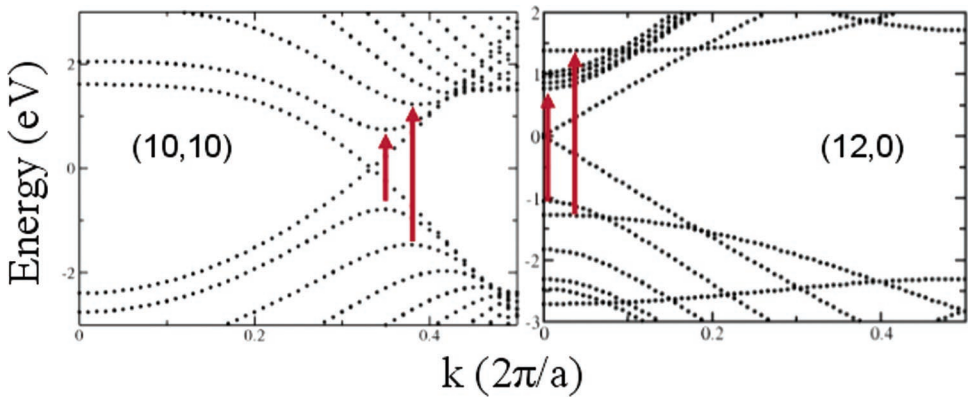

Figure 1. (10,10) and (12,0) SWCNT LDA band structure: The zero of energy is set at the Fermi energy. The solid red arrows indicate the first two allowed optical transitions for light polarized along the tube axis.

exchange-correlation potential[12,13] and using ab initio Troullier−Martins pseudopotentials in the Kleinman−Bylander form.[14,15] The quasiparticle energies are obtained within the GW approximation for the electron self-energy.[7,8,16] We then calculate the two-particle electron−hole excitation energies, wave functions, and optical properties by solving a two-particle Bethe−Salpeter equation (BSE):[6]

$$(E_{ck} - E_{vk})A^S_{vck} + \sum_{k'v'c'} \langle vck|K^{eh}|v'c'k'\rangle A^S_{v'c'k'} = \Omega^S A^S_{vck} \quad (1)$$

where A^S_{vck} is the electron−hole amplitude (or exciton wave function), K^{eh} is the electron−hole interaction kernel, Ω is the excitation energy, and E_{ck} and E_{vk} are the quasiparticle energy of the electron and hole states respectively. The dependence on k in A^S_{vck} represents the contributions from many vertical excitations in k-space that make up the correlated exciton state.

Figure 1 shows the LDA band structure for the (10,10) and (12,0) SWCNTs. Because only light polarized along the tube axis gives a strong optical response,[4,5,17] this polarization is taken for all the optical properties presented below. In this case, the optical perturbation operator transforms under the identity representation in the group of the k-vector, assuming $\vec{q}$ (the wave vector of the incident photon) is vanishingly small. Therefore, the optical transitions obey well-defined selection rules determined by the representations of the group of the k-vector.[18,21] This is a result of the quasi-1D nature of nanotubes (where every k-point lies along the same high-symmetry direction), causing optical transitions to obey well-defined selection rules across entire bands. We find that the first allowed optical transitions in the (10,10) tube occur between the second and third valence subbands (the bands are degenerate) and the second and third conduction subbands (shown by the solid red transition line drawn in Figure 1). The second and third allowed transitions occur between the subsequent sets of valence and conduction subbands.

For the (10,10) and (12,0) tubes, we find the slope in the dispersion relation of the quasiparticle bands increases by approximately 25% when compared to the LDA result. This represents a renormalization of the energy scale for the quasiparticle excitations due to self-energy effects.

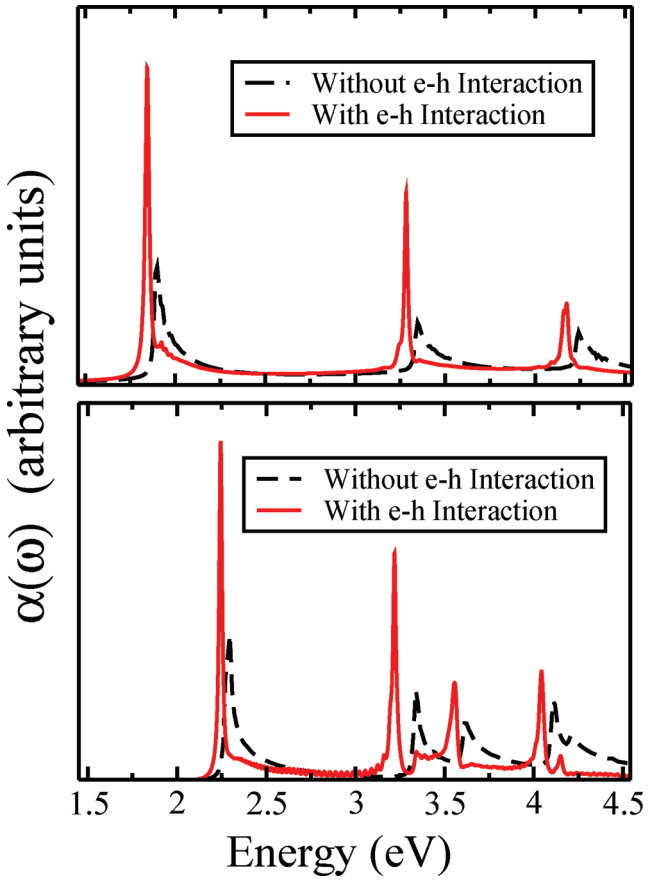

Figure 2. Calculated absorption spectra for the (a) (10,10) and (b) (12,0) tubes for the first several transtions with 20 meV Lorentzian broadening.

Figure 2 shows the optical absorption spectra for the (12,0) and (10,10) tubes over the energy range of the first three optically allowed interband transitions. One can see that each feature is dominated by a single Lorentzian peak followed by a smaller tail characteristic of a 1D van Hove singularity located at the position of the peak in the noninteracting spectrum. To better understand the effect of bound excitons on the absorption line shape, the optical absorption spectra for the first allowed transition (denoted E_{11}) in the (10,10) tube is shown in Figure 3. The actual quantity presented is

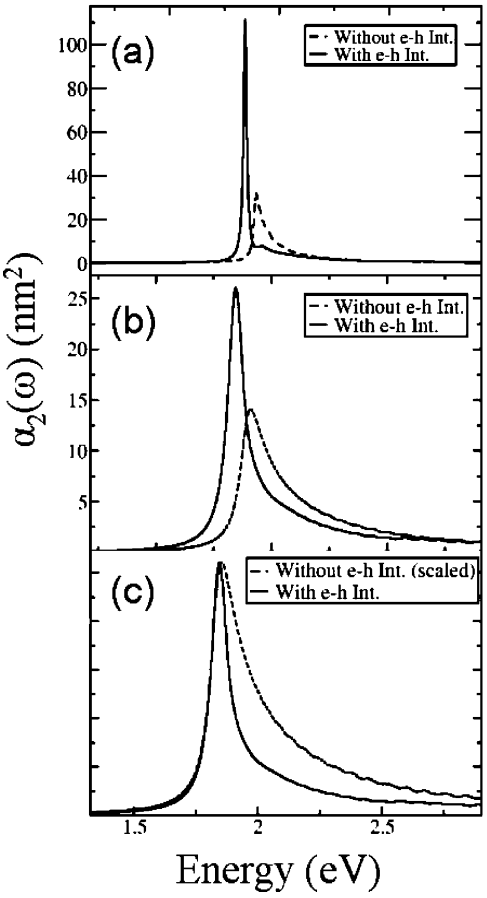

Figure 3. Calculated first absorption peak in the (10,10) SWCNT: with (a) 20 meV and (b) 80 meV Lorentzian broadening. The solid lines include excitonic effects whereas the dashed lines were calculated without the electron−hole interaction included. Only one optically bright bound exciton state is derived from the corresponding van Hove singularity in the JDOS. Panel (c) compares the two spectra each with 80 meV broadening but with the noninteracting spectrum scaled and shifted to match the peak in the interacting case.

$\alpha = \mathrm{Im}\{A(\epsilon - 1)/4\pi\}$, where ϵ is the calculated supercell dielectric function, and A is the cross-sectional area of the supercell perpendicular to the tube axis. The quantity α is the polarizability per tube and, to get a measured polarizability, one should multiply this quantity by the density of tubes per unit area. For each nanotube studied, excitonic effects qualitatively change the spectrum due to the existence of bound exciton states. In the (10,10) tube, the bound exciton associated with the first singularity in the JDOS has a binding energy of 50 meV. In parts a and b of Figure 3, we see that the optical peak arises almost entirely from the single exciton state, showing a profile that is significantly different from the interband transition case. As a comparison, Figure 3c shows the noninteracting spectrum scaled and shifted to match the peak height in the interacting case. We see that the two lineshapes are distinctly different, which should be distinguishable in experiment. For the (12,0) tube, as seen in Figure 2, the first transition is due to a similar bound exciton state with a binding energy of also approximately 50 meV. Although, due to the large screening in metallic tubes, these binding energies are an order of magnitude lower than the typical binding energies in semiconducting SWCNTs of similar diameter, they are still surprisingly large.

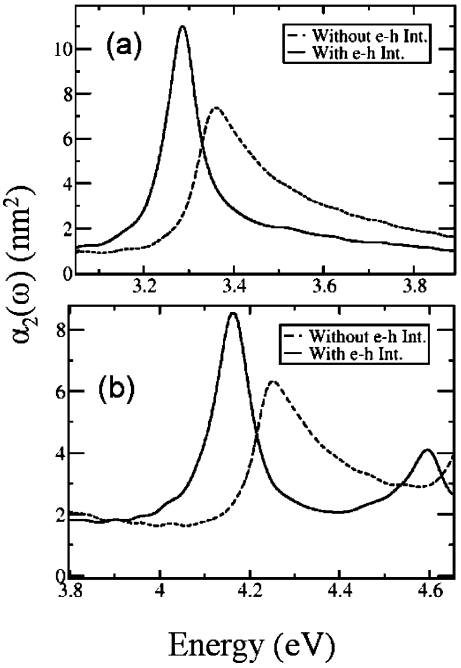

Figure 4. Calculated optical absorption peaks for the (10,10) tube: in the energy range of the (a) E_{22} and (b) E_{33} van Hove singularity in the JDOS. The spectra are arbitrarily broadened by Lorentzians with line widths of 80 meV.

The physics behind why bound exciton states exist at all in the presence of carriers and metallic screening is due to the relative ease of forming bound states in one-dimensional quantum wells and of the existence of optical symmetry gaps in the two-particle spectrum. In one dimension, it has been shown that any potential (other than $V = 0$) that satisfies $\int V(x)\, dx \leq 0$ (i.e., is negative on average) is guaranteed to have at least one bound state.[19,20] In metallic achiral tubes, electron−hole pair excited states formed from the crossing bands are from a different representation of the group of the k-vector[21] than those of optically allowed electron−hole pairs; there is no mixing between those states and the bound exciton states formed from the first optically allowed transitions. Thus, as long as the repulsive exchange term in the electron−hole kernel is weak, a bona fide bound state as calculated is expected. Unlike the case in similar diameter semiconducting tubes, however, our calculations predict only one bright bound exciton state per van Hove singularity and not a series of exciton states.

For the (10,10) tube, the absorption onset is calculated to be at 1.84 eV. The experimental onset has been reported to be 1.75[22] and 1.89 eV.[23,24] For the (12,0) tube, the calculated absorption onset is at 2.25 eV, whereas experimental measurement gives a value of 2.16 eV for the onset.[22,23] Environmental effects like the dielectric screening of the medium are expected to be less important in metallic nanotubes than in semiconducting tubes because of the already comparably high intrinsic dielectric constant of metallic tubes.

Figure 4 shows again the optical absorption spectra for the second and third allowed optical transitions in the (10,10)

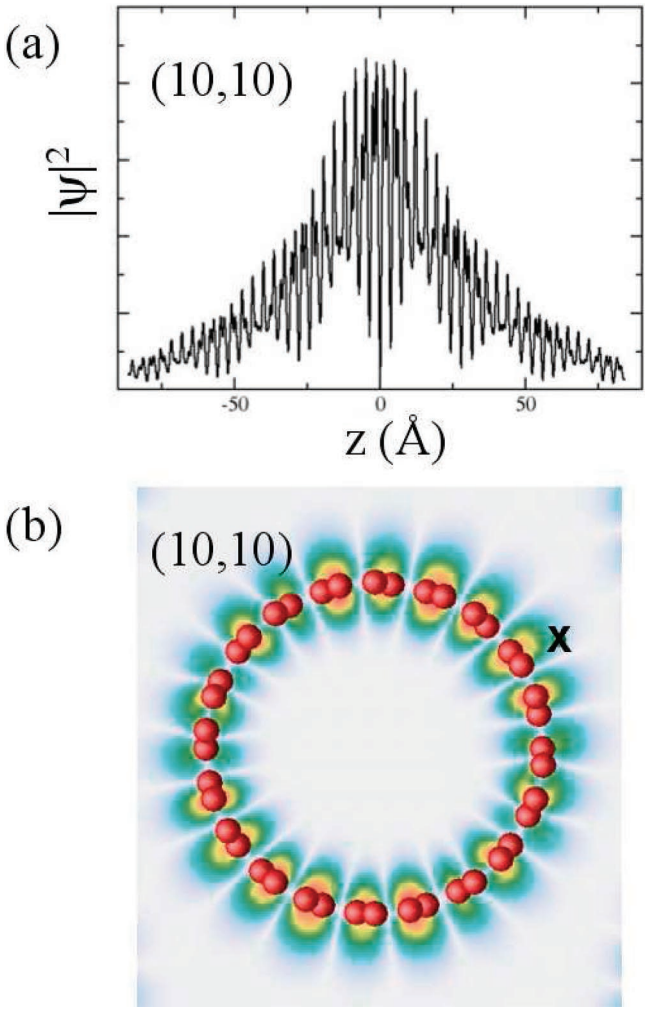

Figure 5. Electron amplitude squared in real space: with the hole position fixed (a) plotted along the tube axis with the hole located at the origin and radial and angular degrees of freedom integrated out and (b) plotted on a cross section of the tube perpendicular to the tube axis. The hole is located at the X in the figure.

tube but with a Lorentzian broadening of 80 meV. We find that a narrow resonant exciton state is responsible for each peak. The E_{22} exciton is a narrow resonance because the electron−hole states from the E_{11} continuum, being of the same symmetry, will mix with E_{22} electron−hole states. However, due to the relatively low value of the JDOS of the E_{11} continuum when compared to that at the E_{22} van Hove singularity, we find that the resonant exciton state is composed of only ∼15% from the E_{11} continuum, making it a very narrow resonance. Thus, we can still identify the binding energy of the resonant exciton states, which is 60 and 50 meV for the second and third transitions, respectively, very similar to that of the E_{11} exciton arising from the first van Hove singularity. For the (12,0) tube, we find a binding energy for E_{22} of 120 meV, more than double the binding energy of E_{11}, due to a significantly greater effective mass, as seen in Figure 1. The binding energy is smaller than that of similar E_{22} bound exciton states in semiconducting tubes but still yields significant effects on the absorption lineshapes.

From the computed electron−hole amplitude, A^S_{vck}, it is found that the bound exciton states for the tubes studied are dominated by a set of degenerate valence and conduction band pairs and peaked in k-space with a width of approximately 1/50 of the Brillouin zone. The electron−hole amplitudes in real space can be determined by expanding in the quasiparticle basis:

$$\Psi(\vec{r}_e,\vec{r}_h) = \sum_{kvc} A_{vck}\phi_{c,k}(\vec{r}_e)\phi^*_{v,k}(\vec{r}_h) \qquad (2)$$

The squared magnitude, $|\Psi(\vec{r}_e,\vec{r}_h = \text{const})|^2$, of this function is shown in Figure 5 for the lowest optically bright bound exciton state of the (10,10) tube with the hole position fixed. The axial spatial extent (analogous to the exciton radius) is approximately 30 Å. This is large compared to an extent of approximately 10−20 Å for similar diameter semiconducting tubes, which is indicative of the smaller exciton binding energy in metallic tubes.

In summary, we confirm the earlier prediction that bound excitons exist in metallic SWCNTs and that excitonic effects are very important in describing the optical properties of metallic nanotubes.[4] In particular, we show that bound excitons exist in the experimentally realizable (10,10) and (12,0) tubes, with binding energies of 50 meV. These exciton binding energies are smaller than those found in semiconducting tubes due to the enhanced screening in metallic tubes. Although the binding energies are small, the calculations show that the optical excitation spectrum is qualitatively altered in character by the excitons and predict several distinct characteristics that may be tested by experiment.

Acknowledgment. This work was supported by National Science Foundation grant no. DMR04-39768 and by the Director, Office of Science, Office of Basic Energy Sciences, Division of Materials Sciences and Engineering Division, U.S. Department of Energy under contract no. DE-AC02-05CH11231. Computational resources have been provided by NSF at the San Diego Supercomputing Center (SDSC) and DOE at the National Energy Research Scientific Computing Center (NERSC). J.D. acknowledges funding from the DOE Computational Science Graduate Fellowship (CSGF).

References

(1) Saito, R.; Fujita, M.; Dresselhaus, G.; Dresselhaus, M. S. *Appl. Phys. Lett.* **1992**, *60*, 2204.
(2) Hamada, N.; Sawada, S.; Oshiyama, A. *Phys. Rev. Lett.* **1992**, *68*, 1579.
(3) Mintmire, J. W.; Dunlap, B. I.; White, C. T. *Phys. Rev. Lett.* **1992**, *68*, 631.
(4) Spataru, C. D.; Ismail-Beigi, S.; Benedict, L. X.; Louie, S. G. *Phys. Rev. Lett.* **2004**, *92*, 077402.
(5) Spataru, C. D.; Ismail-Beigi, S.; Benedict, L. X.; Louie, S. G. *Appl. Phys. A* **2004**, *78*, 1129.
(6) Rohlfing M.; Louie, S. G. *Phys. Rev. B* **2000**, *62*, 4927.
(7) Hybertsen, M. S.; Louie, S. G. *Phys. Rev. B* **1986**, *34*, 5390.
(8) Hybertsen, M. S.; Louie, S. G. *Phys. Rev. Lett.* 1985, *55*, 1418.
(9) Ando, T. *J. Phys. Soc. Jpn.* **1997**, *66*, 1066.
(10) Wang, F.; Dukovic, G.; Brus, L. E.; Heinz, T. F. *Science* **2005**, *308*, 838.
(11) Maultzsch, J.; Romraenke, R.; Reich, S.; Chang, E.; Prezzi, D.; Ruini, A.; Molinari, E.; Strano, M. S.; Thomsen, C.; Lienau, C. *Phys. Rev. B* **2005**, *72*, 241402(R).

(12) Louie, S. G. *Conceptual Foundations of Materials: A Standard Model for Ground- and Excited-State Properties*; Contemporary Concepts of Condensed Matter Science; Elsevier: New York, 2006.
(13) Kohn, W.; Sham, L. J. *Phys. Rev. A* **1965**, *140*, 1133.
(14) Troullier, N.; Martins, J. L. *Phys. Rev. B* **1991**, *43*, 1993.
(15) Kleinman, L.; Bylander, D. M. *Phys. Rev. Lett.* **1982**, *48*, 1425.
(16) Hedin, L. *Phys. Rev. A* **1965**, *139*, 796.
(17) Ajiki, H.; Ando, T. *Physica B* **1994**, *201*, 349.
(18) Delaney, P.; Choi, H. J.; Ihm, J.; Louie, S. G.; Cohen, M. L. *Phys. Rev. B* **1999**, *60*, 7899.
(19) Kocher, C. A. *Am. J. Phys*. **1977**, *45*, 71.
(20) Simon, B. *Ann. Phys*. **1976**, *97*, 279.
(21) Barros, E. B.; Capaz, R. B.; Jorio, A.; Samsonidze, G. G.; Souza Filho, A. G.; Ismail-Beigi, S.; Spataru, C. D.; Louie, S. G.; Dresselhaus, G.; Dresselhaus, M. S. *Phys. Rev. B* **2006**, *73*, 241406.
(22) Strano, M.; Doorn, S.; Haroz, E.; Kittrell, C.; Hauge, R.; Smalley, R. *Nano Lett.* **2003**, *3*, 1091.
(23) Fantini, C.; Jorio, A.; Souza, M.; Strano, M. S.; Dresselhaus, M. S.; Pimenta, M. A. *Phys. Rev. Lett*. **2004**, *93*, 147406.
(24) Barone, V.; Peralta, J.; Scuseria, G. *Nano Lett.* **2005**, *5*, 1830.

NL070577F